POLARIZATION SINGULARITIES IN THREE-DIMENSIONAL OPTICAL FIELDS: THE NEXT FRONTIER

I. FREUND

Physics Department, Bar-Ilan University
(Ramat-Gan 52900, Israel)

UDC 535.215

Polarization singularities are studied in simulated elliptically polarized, three dimensional random wave fields. The coherency matrix is shown to provide a highly useful tool for the study of singular points of circular polarization, C points, and singular points of linear polarization, L points. Both types of points are organized into continuous lines, C lines and L lines, respectively, that meander throughout the field. These lines were traced out by tracking zeros of appropriate discriminants of the characteristic equation of the coherency matrix. The ellipse winding number of a singularity (C or L point) was defined in terms of the rotation of the polarization figures surrounding the singularity. Using the eigenvalues and eigenvectors of this matrix, together with a complex Stokes field representation of the singularities, sign inversions of the ellipse winding number of C points were found on C lines, and switches in ellipse winding number of L points were found on L lines. The former finding is in accord with the current theory, the latter is not encompassed by any current theory. A qualitative explanation of these findings is presented.

Introduction

Although the basic theory of polarization singularities was developed some two decades ago [1—6], and important aspects confirmed experimentally using microwaves [7, 8], it is only very recently that a practical method for the study of such singularities in the optical region was developed under the leadership of Prof. Marat Soskin [9, 10], to whom this paper is dedicated.

There are two basic types of polarization singularities: C points, which are points of circular polarization, and L points, which are points of linear polarization. In general, C points and L points are embedded in a field of elliptical polarization, and exert a remarkable influence on the surrounding polarization ellipses. In two dimensional ($2D$), or paraxial, fields, C points are isolated points in the plane, here the xy-plane, whereas L points are organized into continuous lines in the plane that separate regions of right and left handed elliptical polarization. The presence of a C point forces the surrounding ellipses to rotate about the point with a topological winding number that is generically $\pm 1/2$. As the xy-plane is translated along the propagation direction, here the Z-axis, C points trace out a line of circular polarization, whereas L points trace out a surface of linear polarization, an L surface. In addition to these singularities, it has very recently been found that paraxial fields exhibit polarization stationary points, extrema (maxima and minima), and saddle points [11]. Collectively, polarization singularities and stationary points are called polarization critical points, and the experimental challenge was to find a practical method for the measurement of these critical points. This task was undertaken by Prof. Soskin and his students who, building on recent theoretical calculations [12, 13], initiated the development of, and brought to perfection, a method that offers unprecedented resolution and accuracy, a method they called Singular Stokes Polarimetry (SSP). Applying their new experimental method to different systems, Prof. Soskin and his students discovered an astounding variety of polarization structures [10], structures whose complexity and richness far surpass anything considered previously by theory [1—6], or seen in computer simulations [11] or microwave experiments [7, 8].

SSP opens the door to the study of polarization singularities in $2D$ fields, and will undoubtedly lead to many additional important scientific discoveries, as well as practical applications. With the theoretical and experimental basis for the study of $2D$ fields now well in hand, the next frontier, both theoretically and experimentally, becomes the study of polarization singularities in $3D$ fields.

In $3D$, C points are organized into continuous lines, C lines. Similarly, and unlike the case of $2D$, in $3D$, L points form lines, not surfaces. In the transition from $3D$ to $2D$, an L line grows into a surface as the ellipses in the vicinity of the line become ever narrower, asymptotically collapsing to lines (linear polarization). In this process, regions of right and left handed polarization become segregated and bounded by L surfaces. The details of this transformation, the growth of $2D$ stationary points, the detailed properties of C and L lines, and many other

properties of $3D$ fields, still remain to be elucidated. Random fields provide a useful test ground for study of the above phenomena, because anything that can happen most likely will happen in such fields. Random fields, however, are too complex for the most part to be studied in detail analytically, although certain statistical properties of the field may be calculated [14, 15].

There is at present no practical, general method described in the literature for tracing out C lines and L lines in complex $3D$ fields, let alone for examining the detailed properties of these lines. Here we describe such a method, and use it to examine C lines and L lines in computer simulations of random $3D$ fields. In addition to verifying, for the first time, important predictions of the current theory [1, 5], we find new phenomena not encompassed by any theory.

1. The $3D$ Coherency Matrix and the Complex $2D$ Stokes Field

The elements E_{ij} of the symmetric 3×3 real coherency matrix $\mathcal{M}$ of a $3D$ optical field are here defined by

$$E_{ij} = \mathrm{Re}(E_i E_j), i, j = x, y, Z, \tag{1}$$

where the E_i are components of the electric field vector $\mathbf{E}$ along the orthogonal coordinates axes x,y,Z. The eigenvalues λ_k, k = 1,2,3 of $\mathcal{M}$ are solutions of its characteristic equation,

$$\lambda^3 + a_1\lambda^2 + a_2\lambda + a_3 = 0. \tag{2}$$

These eigenvalues are positive definite, are here ordered by increasing value, are normalized by the largest, $\lambda_1 \leq \lambda_2 \leq \lambda_3 = 1$, and the corresponding eigenvectors are here labeled $\mathbf{V}_1$, $\mathbf{V}_2$, $\mathbf{V}_3$.

In the monochromatic optical fields of interest here, the polarization ellipses are planar [16], and $\lambda_1 = 0$, which makes $a_3 = \lambda_1\lambda_2\lambda_3 = 0$. Under these circumstances, Eq. (2) reduces to a quadratic one. At a C point, $\lambda_2 = \lambda_3$, and such points may be located using zeros of the discriminant

$$\mathcal{D}_C = a_1^2 - 4a_2. \tag{3}$$

At an L point, $\lambda_2 = 0$, and such points may be located using zeros of the discriminant

$$\mathcal{D}_L = a_2. \tag{4}$$

For each singular point, there is a *proper line of sight* (LOS). For C points, the LOS is normal to the plane of the C point. This direction corresponds to $\mathbf{V}_1$. When viewed down this LOS, the polarization figure is seen as a circle, and theory predicts that the surrounding ellipses rotate should about this circle with generic winding number $\pm 1/2$ [1,5]. For L points, the proper LOS is down the line of oscillation of $\mathbf{E}$, i.e. along $\mathbf{V}_3$. When viewed down this direction, the polarization figure of an L point is seen as a point, and here theory predicts that the surrounding (thin) ellipses rotate about this point with generic winding number ± 1 [1,5]. For both types of polarization singularity, these predictions are, for a plane, oriented normal to the proper line of sight, the *proper plane*. For C points, the proper plane is the plane of the circle; for L points, the proper plane contains the point and is oriented normal to the proper LOS. In what follows, we examine the polarization ellipses in the proper plane when viewed down the proper LOS: we call the field that is seen in this way the *proper field*.

The circular polarization figures on an C line, and the linear figures on an L line, can make arbitrary angles with respect to the line. The same is true for the surrounding ellipses. Thus, the proper field is a projection down the proper LOS onto the proper plane of the central singularity and its surrounding ellipses. Because the projection of an ellipse is also an ellipse, the proper field is a field of planar ellipses, i.e. a $2D$ field.

We label orthogonal axes in the plane of the proper field by x',y', and the corresponding field components by E'_x,E'_y. The azimuthal angle α that the long axis of an ellipse makes with the x'-axis is given by [16]

$$2\alpha = \mathrm{atan2}(S_2, S_1), \tag{5}$$

where atan2 is the two argument (four quadrant) arctangent, and the Stokes parameters are defined by

$$S_1 = |E'_x|^2 - |E'_y|^2, \; S_2 = 2\mathrm{Re}(E'_x * E'_y). \tag{6}$$

It is useful to form the complex Stokes field [12,13]

$$S_{12} = S_1 + iS_2 = A_{12}\exp(i\Phi_{12}), \tag{7a}$$

$$\Phi_{12} = \mathrm{atan2}(S_2, S_1) = 2\alpha, \tag{7b}$$

because then the C points and L points of the proper field are vortices of the Stokes phase Φ_{12}. Because of the factor of 2 in the R.H.S. of Eq. (7b), these Stokes vortices have generic winding numbers that are twice those of the corresponding polarization singularity, i.e. ± 1 for C points, ± 2 for L points.

The Stokes vortices lie at the intersections of the zero crossings Z_1 of S_1 and Z_2 of S_2. From the rules of the phase ratchet [17], a single Z_1 and a single Z_2 intersect at a C point, whereas at an L point a pair of Z_1 and a pair of Z_2 intersect with cardinal ordering $Z_1Z_2Z_1Z_2$.

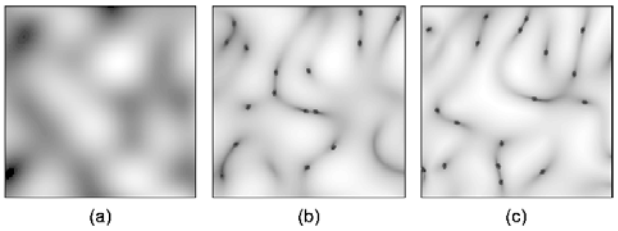

Fig. 1. Simulated random field. Shown is the xy-plane at $Z = 0$ over the region $(\Delta x, \Delta y) = (\pm 10, \pm 10)$. Increasing amplitudes are coded black to white. a — speckle intensity (the low contrast matches that expected for a randomly polarized ellipse field). b — C line discriminant $\mathcal{D}_C$, Eq. (3). c — L line discriminant $\mathcal{D}_L$, Eq. (4). The black areas in Fig. b, (c) correspond to the intersection of C lines (L lines) with the xy-plane. At these points, here emphasized for clarity, the amplitude of the discriminant vanishes

From the phase ratchet rules, it also follows that if the ordering of zero crossings at an L point is $Z_1 Z_2 Z_2 Z_1$, or $Z_2 Z_2 Z_1 Z_1$, etc., i.e. the ordering differs from the cardinal ordering or a cyclic permutation thereof, then the winding number of the vortex, and therefore of the L point, is zero.

2. Random Field Simulation

The simulated random wave field studied here consists of a large number of linearly polarized waves whose wavevectors $\mathbf{k}$ all have unit length, and have random directions such that the half space $Z > 0$ is approximately filled over the region $-1/\sqrt{3} < k_x, k_y < +1/\sqrt{3}$. The limiting values $\pm 1/\sqrt{3}$ were used for simplicity to keep $k_Z = (1 - k_x^2 - k_y^2)^{1/2}$ pure real. The projections E_x and E_y of $\mathbf{E}$ were randomly distributed in the xy-plane, and the divergence condition was used to fix E_Z via $E_x k_x + E_y k_y + E_Z k_Z = 0$.

With the above scaling, the spread in propagation directions is approximately 70°, and the characteristic distance over which changes in the transverse wave field occur, i.e. the transverse coherence length, is of order 2π. The speckle pattern of a typical realization is shown in Fig. 1,a: its low contrast is in accord with expectation for a randomly polarized ellipse field. The corresponding C point discriminant $\mathcal{D}_C$ is shown in Fig. 1,b, the L point discriminant $\mathcal{D}_L$ in Fig. 1,c.

3. C Lines

C lines were traced out in $3D$ using zeros of $\mathcal{D}_C$. Using double precision, 64 bit arithmetic, the program employed calculates $\mathcal{D}_C$ within a small area surrounding some preselected point in the xy-plane at some initial value of Z, and finds the near zero minimum of $\mathcal{D}_C$ within this area. The field is then recalculated on an expanded scale about this initial minimum, and a better estimate of its location is obtained. This process is repeated until the coordinates of the minimum are stationary to $\pm 10^{-5}$ (typically 3—10 iterations). Attempts at further refinement failed due to rounding errors that were induced by the large number of steps needed to calculate the field at a given point. After storing the coordinates of the C point, Z was incremented and the procedure repeated until either a predetermined range in Z was covered, or the C line curved back on itself. Every C line studied ultimately did this, implying that C lines form closed loops rather than endless lines that meander throughout the wave field. Fig. 2,a displays a segment of a typical C line. After obtaining the coordinates of typically some 3,000—10,000 closely spaced C points on the line, the eigenvalues and eigenvectors of $\mathcal{M}$ were then calculated. With the largest eigenvalue, λ_3, normalized to 1, typically the smallest eigenvalue, λ_1, was of order 10^{-17} (i.e. essentially zero), and $\lambda_3 - \lambda_2 \sim 10^{-5}$ (i.e. effectively degenerate).

An important theoretical prediction not previously tested involves the location of points on a C line at which inversion of the sign of the C point winding number occurs. The theoretical prediction is that such an inversion takes place at a point where the proper line of sight, $\mathbf{V}_1$, is perpendicular to the C line, and in generic fields only at such a point. Fig. 2,b shows a plot of the angle θ between $\mathbf{V}_1$ and the tangent to the C line shown in Fig. 2,a. As may be seen, there is a point in this figure where $\theta = 90°$. Fig. 3 shows the field in the vicinity of this point. Figs. 3,a,b show the Stokes phase and zero crossings, just before this point, and Figs. 3,c,d show the field right after. Sign inversion of the Stokes (ellipse) winding number from -1 to $+1$ ($-1/2$ to $+1/2$) upon passing through $\theta = 90°$ is clearly evident, in full accord with theory [1, 5]. At $\theta = 90°$ (not shown), the sign inversion point itself, Z_1 and Z_2 overlap, and the winding number becomes indeterminate, in accord with theory. These observations appear to be the first confirmation of the theoretical predictions regarding sign inversion.

We close this section by noting that we find sign inversion at *every* point where $\theta = 90°$ on a *every* C line studied, and do not find sign inversion at any other points on C lines, so that our simulation fully confirms the current theory of C lines [1, 5]. The situation is quite different, however, for L lines.

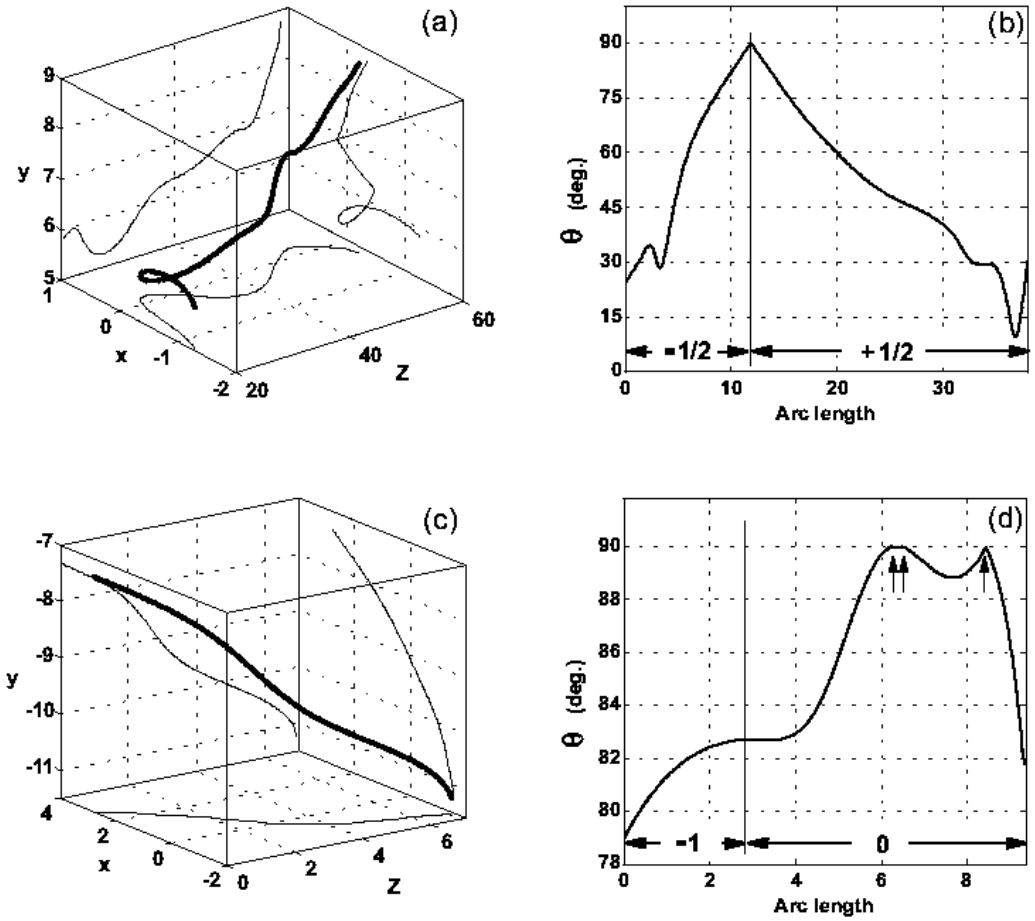

Fig. 2. C lines, L lines, and ellipse winding number switchovers. a — C line. b — angle θ between the proper line of sight and the tangent to the C line in Fig.a as a function of distance (arc length) along the line (the winding number of the C point switches from $-1/2$ to $+1/2$ at the point on the line where $\theta = 90°$). c — L line. d — θ vs. arc length for the L line in Fig.c. The vertical arrows show three points on the line at which $\theta = 90°$. The winding number does not switch at these points, but rather switches from -1 to 0 at an arc length approximately equal to 3

4. *L* lines

L lines were traced out in the same manner as C lines, except that here the discriminant was $\mathcal{D}_L$, Eq. (4). Also these lines were found to form closed loops. Fig. 2,c displays a segment of a typical L line. On the line, the normalized eigenvalues λ_1 and λ_2 are typically of order $10^{-17}(\lambda_3 = 1)$.

Here we define the winding number of an L point in terms of the rotation of the (thin) ellipses surrounding the point (the ellipse winding number). This definition is the same as that used in [1, 5] for C points, but differs from the definition used in [1, 5] for L points, where the L point winding number is defined in terms of the rotation of ellipse normals (the normal winding number).

The current theory of the normal winding number for L lines [1, 5] predicts the following: (i) At all points on the line where $\mathbf{V}_3$, the direction of linear polarization, is not perpendicular to the line, the winding number of the ellipses surrounding the L point should be ± 1 in generic fields (the winding number of the corresponding Stokes vortex is then ± 2). (ii) At points where $\mathbf{V}_3$ is perpendicular to the line, and only at these points, the winding number becomes indeterminate. (iii) Upon passing through these points of indeterminate winding number, the sign of the winding number, inverts.

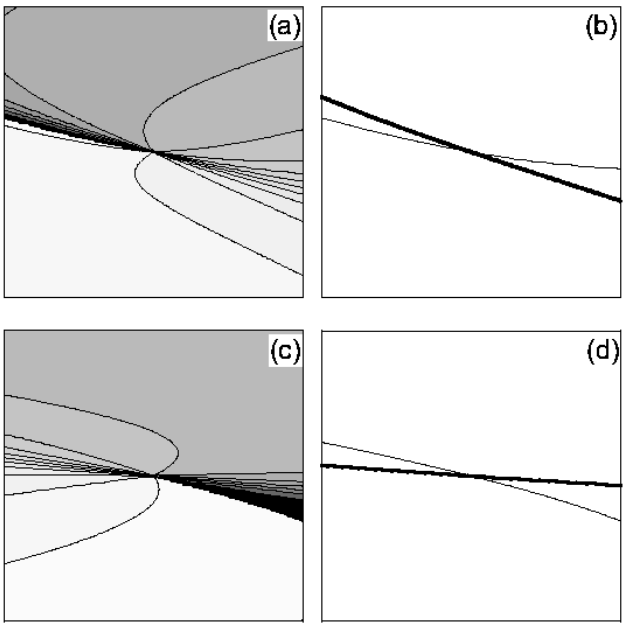

Fig. 3. C point sign inversion. Stokes field corresponding to the C line in Figs. 2,a, b at points in the immediate vicinity of the switchover point at $\theta = 90°$. Here, the Stokes phase is coded $-\pi$ to $+\pi$ black to white (a, c), zero crossing Z_1 (Z_2) is shown by a thick line (thin line) (b, d), field just before the switchover (a, b), field after the switchover (c, d). a — starting at the black sector, along a path that encircles the vortex, the phase may be seen to circulate (increase) uniformly by 2π in the negative, clockwise, direction, and the Stokes vortex (ellipse field C point) has winding number -1 $(-1/2)$. c — the phase circulates uniformly by 2π in the positive, counterclockwise, direction, and the Stokes vortex (ellipse field C point) has winding number $+1$ $(+1/2)$. The inversion in the ordering of Z_1 and Z_2 in going from b to c reflects the change in sign of the winding number. At the switchover point itself, $\theta = 90°$ (not shown), Z_1 and Z_2 overlap and the winding number is indeterminate

For the ellipse winding number, however, our simulations differ from the predictions given above for the normal winding number, and we find: (i) Every L line examined is divided into long segments on which the winding number alternates between 0 and ± 1 for the ellipse field (0 and ± 2 for the Stokes field). (ii) At the boundary between these regions, the winding number becomes indeterminate, and the angle between $\mathbf{V}_3$ and the L line is *arbitrary* at these boundary points. (iii) The sign of the winding number does not necessarily invert upon passing through a region with zero winding number.

Fig. 2,d shows the angle θ between $\mathbf{V}_3$ and the L line in Fig. 2,c. The winding number of each line segment is also shown. As may be seen, there is a point on the L line at which the winding number switches from -1 to zero. Figs. 4,a, b shows the Stokes phase field, and S_1 and S_2 zero crossings (Z_1, Z_2), just before the winding number switches, Figs. 4,c, d show the field just after the switch. The change in the ordering of zero crossings that causes the switchover to occur is clearly evident, in accord with the rules of the phase ratchet discussed above [17]. At the switchover point itself (not shown), Z_1 and Z_2 overlap, and the winding number is indeterminate.

5. Discussion

Although a detailed theory of the above phenomena will be reported on separately, we give here a qualitative discussion of the results obtained using the very different properties of the Stokes vortices corresponding to C points and to L points.

At a C point, the corresponding Stokes vortex has unit charge and is located where a single Z_1 intersects a single Z_2. Moving, say, clockwise on a path that surrounds the vortex, let the zero crossing sequence be $Z_1 Z_2$. As an inversion point on a C line is approached, the angle between these zero crossings decreases towards zero, say because Z_1 rotates towards Z_2. At the inversion point itself, the zero crossings overlap. The winding number becomes indeterminate at this point because, on every path that intersects these overlapping zero crossings, the winding number jumps discontinuously by $\pm\pi/2$ with indeterminate sign [18]. Such a point is obviously unstable, and Z_1 continues to rotate as one moves along the C line. The zero crossing sequence therefore becomes $Z_2 Z_1$, and inversion of the vortex sign occurs. Thus, for stable C points, there are only two choices available to the winding number, ± 1.

The situation is very different, however, for an L point which has Stokes winding number ± 2. Here the initial zero crossing sequence is say $Z_1 Z_2 Z_1 Z_2$ [17]. Let the winding number be $+2$. As one moves along the L line, also let Z_1 rotate towards Z_2. At the boundary between a zero and nonzero index, the two zero crossings overlap, and after moving past this boundary, the sequence becomes $Z_2 Z_1 Z_1 Z_2$. This sequence corresponds to zero winding number [17]. The winding number remains zero until either Z_1 rotates past the last Z_2, establishing the sequence $Z_2 Z_1 Z_2 Z_1$, with winding number -2, i.e. sign inversion occurs, or else, Z_1 reverses its rotation direction and returns to its starting position, in which case the winding number is once again $+2$. A stable winding number of ± 1 is not possible with four

zero crossings [17], and so never occurs in the above sequence.

Assuming all zero crossing configurations are equally probable, there are twice as many ways of obtaining zero winding number as there are ways of obtaining a non zero winding number. Starting with say Z_1, only one sequence, $Z_1Z_2Z_1Z_2$, yields a non zero winding number (± 2), whereas the sequence $Z_1Z_1Z_2Z_2$ and the sequence $Z_1Z_2Z_2Z_1$ both yield zero winding number [17]. The observation that L line segments with zero winding number are substantially more likely than those with nonzero winding number is in accord with these considerations.

In $3D$ fields, the sign σ of a singularity is given by $\sigma = \mathrm{sign}(\mathbf{V}\cdot\mathbf{J})$, where $\mathbf{V}$ is a unit vector along the line of sight, and $\mathbf{J}$ is an appropriately defined topological current [14, 15]. An indeterminate winding number requires $\sigma = 0$. Now, a generic C point corresponds to a first order vortex in one of the circularly polarized components of the field [1, 2]. For such a point, $\mathbf{J} = 0$ requires an unstable, and therefore nongeneric, osculation of the zero surfaces of the real and imaginary parts of the wave function of this component (in a plane, the overlap of real and imaginary zero crossings). Because generically $\mathbf{J}$ does not vanish, $\sigma = 0$ requires $\mathbf{V}$ be perpendicular to $\mathbf{J}$. This is the generic condition for an inversion point on a C line [1, 5]. As $\mathbf{V}$ rotates through the inversion point, $\mathbf{V}\cdot\mathbf{J}$ and therefore σ, change sign. But for an L point, the region of the parameter space corresponding to $\mathbf{J} = 0$ (i.e. a zero crossing ordering that produces zero winding number) exceeds the region of nonzero $\mathbf{J}$. Thus, on L lines, the winding number switches due to a change in $\mathbf{J}$ itself, and not because $\mathbf{V}$ is perpendicular to $\mathbf{J}$. Our simulations show that such changes in $\mathbf{J}$ can occur anywhere along an L line.

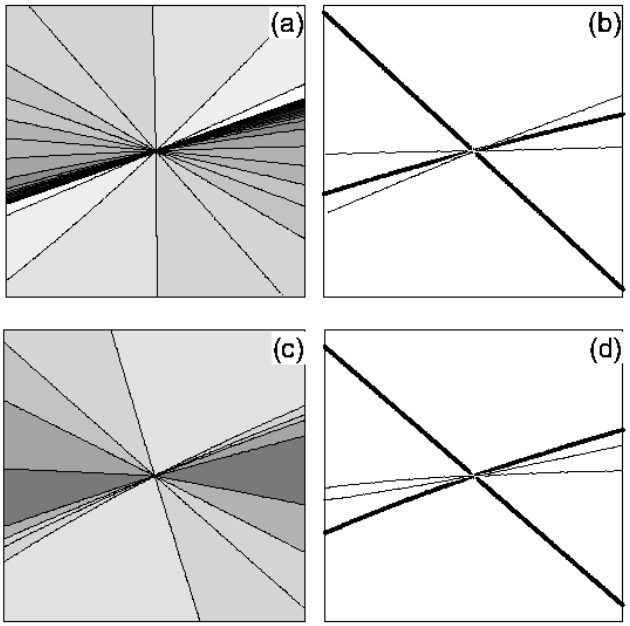

Fig. 4. L point ellipse winding number switchover. Stokes field corresponding to the L line in Figs. 2,c,d at points in the immediate vicinity of the switchover point at an arc length of ~ 3. Here, the Stokes phase is coded $-\pi$ to $+\pi$ black to white (a, c), and zero crossings Z_1 (Z_2) are shown by thick (thin) lines (b, d), field just before the switchover (a, b). a — starting at a black sector, along a path that encircles the vortex the phase, which is folded back into the region $-\pi$ to $+\pi$, may be seen to circulate (increase) uniformly in the negative, clockwise, direction by 4π, and the Stokes vortex (ellipse field L point) has winding number -2 (-1). b — in the upper half plane the zero crossings $Z_1$and Z_2 have ordering $Z_1Z_2Z_1Z_2$, corresponding to Stokes winding number -2 in Fig. a (c, d — field after the switchover). c — starting at the darkest sector of the figure, the phase may be seen to circulate in both the positive, counterclockwise, direction, *and* the negative, clockwise, direction, indicating a net winding number of zero. d — in the upper half plane the zero crossings Z_1 and Z_2 have ordering $Z_1Z_1Z_2Z_2$, corresponding to the Stokes winding number 0 in Fig.c. At the switchover point itself (not shown), Z_1 and Z_2 overlap and the winding number is indeterminate

Summary

Both the coherency matrix $\mathcal{M}$, Eq. (1), and the complex Stokes field S_{12}, Eqs. (7), were shown to be extremely useful theoretical tools for the study of $3D$ ellipse fields. Using zeros of the discriminants of $\mathcal{M}$, Eqs. (3, 4) and Fig. 1,c lines, Fig. 2,a, and L lines, Fig. 2,c, were traced out in simulated generic random fields. The eigenvalues and eigenvectors of $\mathcal{M}$ were calculated along the lines, and one eigenvalue was found to be essentially zero in all cases, in accord with theoretical expectation for an ellipse field [16]. For all points on a C line, two nonzero eigenvalues were always found to be effectively degenerate, also in accord with theory. For all points on an L line, two zero eigenvalues, and one nonzero eigenvalue, were always found, again in accord with theory. On C lines, the winding number was found to be $\pm 1/2$, in accord with theory [1, 5]. On L lines, the ellipse winding number was found to be either ± 2, or zero, the former (± 2) being in accord with the theory of the normal winding number [1, 5], the latter (0) not encompassed by any previous theory. The angle between the proper line of sight and the C or L line

was calculated, Figs. $2, b, d$. Sign inversion was observed on C lines at points where this angle is $90°$, in accord with theory [1, 5]. In contrast, on L lines, the winding number was found to switch between ± 2 and zero at arbitrary points on the line, a behavior not encompassed by any available theory. A qualitative theory of the above differences between C and L lines was described, a quantitative theory will be presented elsewhere.

The ball, as it were, is now passed to the court of the experimentalists. The experimental problems associated with measurements in $3D$ optical fields are undoubtedly severe, but considering the rapid pace of past successes, one can anticipate that these problems will be solved in time for the next special issue of this journal.

The many pioneering studies of Prof. Marat S. Soskin and his colleagues over the past decade have been a major driving force in the rapid development of the new field of Singular Optics: I am most pleased to acknowledge the many personal discussions and numerous emails that have served as a source of inspiration and enlightenment, and that have contributed importantly to my own work. For the present study, I am also pleased to acknowledge a useful suggestion by Prof. David Kessler, and email correspondence with Sir Michael Berry, Prof. John Nye and Dr. Mark Dennis.

1. *Nye J.F.* Natural Focusing and the Fine Structure of Light. — Bristol: IOP Publ., 1999.
2. *Nye. J.F.* // Physics of Defects/Ed. by R. Balian, M. Kleman, and J.P. Poirier. — Amsterdam: North-Holland, 1981. — P. 545—549.
3. *Nye J.F.* //Proc. Roy. Soc. Lond. A.— 1983.— **387**. — P. 105—132.
4. *Nye J.F.*// Ibid. — **389**. — P. 279—290.
5. *Nye. J.F., Hajnal J.V.*// Ibid. —1987. — **409**. — P. 21—36.
6. *Hajnal J.V.*// Ibid. — **414**. — P. 433—446.
7. *Hajnal J.V.*// Ibid.— P.447—468.
8. *Hajnal J.V.*//Ibid. —1990. — **430**. — P.413 — 421.
9. *Soskin M.S., Denisenko V., Freund I.*//Opt. Lett. — 2003. — **28**. — P. 1475—1477.
10. *Soskin M.S., Denisenko V., Egorov R.*// JOSA (to be published).
11. *Freund I., Soskin M.S., Mokhun A.I.*//Opt. Communs.— 2002.— **208**. — P. 223—253.
12. *Konukhov A.I., Melnikov L.A.*//J. Opt. B.—2001. — **3**. — P.S139—S144.
13. *Freund I.* // Opt. Lett. — 2001. — **26**. — P.1996—1998.
14. *Berry M.V. Dennis M.R.*// Proc. Roy. Soc. Lond. A. — 2001. — **457**. — P.141—155.
15. *Dennis. M.R.*// Opt. Communs. — 2002. — **213**. — P. 201—221.
16. *Born M. Wolf E.W.* Principles of Optics. — Oxford: Pergamon Press, 1959.
17. *Freund I.*// Opt. Communs. — 1999. —**159**.— 99—117.
18. *Freund I.* //Ibid. — 2002. — **201**.— P. 251—270.

ПОЛЯРИЗАЦІЙНІ СИНГУЛЯРНОСТІ В ТРИВИМІРНИХ ОПТИЧНИХ ПОЛЯХ: НОВИЙ РУБІЖ

І. Фройнд

Р е з ю м е

Вивчаються поляризаційні сингулярності в модельованих еліптично поляризованих тривимірних випадкових хвильових полях. Показано, що матриця когерентності є дуже корисним інструментом для дослідження сингулярних точок циркулярної поляризації, C-точок, та сингулярних точок лінійної поляризації, L-точок. Обидва типи точок організуються в неперервні лінії, C- та L-лінії відповідно, які пронизують поле. Ці лінії було знайдено за допомогою відслідковування нулів відповідних визначників характеристичних рівнянь матриці когерентності. За допомогою власних значень та власних векторів цієї матриці разом з зображенням сингулярностей у вигляді комплексного стоксова поля були знайдені знакові інверсії індексу кручення C-точок на C-лінії, а також були встановлені зміни в індексі кручення L-точок на L-лінії. Перші розв'язки узгоджуються з сучасною теорією, другі — не забезпечуються жодною з сучасних теорій. Дано якісне пояснення цих розв'язків.